Contents lists available at ScienceDirect

## Microchemical Journal

journal homepage: www.elsevier.com/locate/microc





## In situ monitoring of neurotransmitters using a polymer nanostructured electrochemical sensing microchip

Md Fazlay Rubby <sup>a</sup>, Catharine Fonder <sup>b</sup>, Sajid Uchayash <sup>a</sup>, Shafayet Ahmed Siddiqui <sup>b</sup>, Ian Schneider <sup>c,d</sup>, Donald S. Sakaguchi <sup>b,d,e</sup>, Long Que <sup>a,\*</sup>

- <sup>a</sup> Department of Electrical and Computer Engineering, Iowa State University, Ames, IA 50011, USA
- b Molecular, Cellular, and Developmental Biology Program, Iowa State University, Ames, IA 50011, USA
- Department of Chemical and Biological Engineering, Iowa State University, Ames, IA 50011, USA
- <sup>d</sup> Department of Genetics, Development and Cell Biology, Iowa State University, Ames, IA 50011, USA
- e Neuroscience Program, Iowa State University, Ames, IA 50011, USA

#### ARTICLE INFO

## Keywords: Polymer nanostructured electrodes Electrochemical sensing microchip Multiplexed detection

Neurotransmitter monitoring

Real-time detection

#### ABSTRACT

Neurotransmitters are used by the nervous system to transmit messages between neurons. The abnormal levels of the neurotransmitters may lead to neurological disorders. It is very important to monitor their levels in patients. Herein, we report a polymer nanostructured electrodes-enabled electrochemical sensing microchip for detecting dopamine and serotonin. The nanostructures on the electrode can enhance the surface area of the electrode dramatically. As a result, the measured electrical signals increased in comparison with those of an electrochemical sensor with an electrode of a flat surface. It has been found that this microchip can detect neurotransmitters with a level as low as ~ 120 nM with high specificity and can be used to monitor the dopamine and serotonin in a mixed sample successfully in both static and dynamic conditions. Finally, the real-time measurements of dopamine released from N27-A dopaminergic neural cells using the microchip have been demonstrated.

## 1. Introduction

Neurotransmitters such as dopamine and serotonin serve as messenger chemicals among neuron cells in the human nervous system to maintain important physiological functions of the brain and other related body parts involved in sensing, expression, and action [1-3]. It has been well known that for many psychiatric disorders, neurotransmitters and their receptors play a major role in pathogenesis [4–5]. For instance, the dopamine neurotransmission system in the central nervous system (CNS) is crucial for a myriad of physiological functions, including the control of movement and emotions, as well as cognitive functions. A considerable number of neurological and psychiatric disorders have been associated with dysfunctions of one or more of the dopaminergic neurotransmission pathways and thus abnormal levels of dopamine. Among these disorders are Parkinson's disease (PD), schizophrenia, attention-deficit/hyperactivity disorder (ADHD), and addiction. Although serotonin cannot be transported across the blood-brain barrier, anomalous whole-blood serotonin levels are correlated with clinical depression [6-8], and timely intervention in a personalized medicinebased setting can significantly reduce the associated medical and socioeconomic burdens [9-10]. Furthermore, serotonin is involved in steering numerous behavioral and physiological functions, and abnormalities in serotonin levels are also found in patients with hypertension [11] and gastrointestinal disorders such as irritable bowel syndrome (IBS) [12]. Monitoring and regulating the levels of these neurotransmitters is therefore essential not only for understanding signal communication pathways and functions of our nervous system but also for diagnostics and treatment of many brain-related diseases [4-10,13-16]. In particular, the balance between neurotransmitters such as dopamine and serotonin is of important significance when developing novel treatments or medications [15-16].

The main technique for detecting neurotransmitters in patients' samples is based on high-performance liquid chromatography (HPLC) as, in contrast to other techniques, it can selectively discriminate between different neurotransmitters [17–19]. However, HPLC suffers from financial drawbacks, as it requires sophisticated equipment that needs to be used in a lab environment. Another popular technique used for neurotransmitter detection in humans is positron emission tomography

E-mail address: lque@iastate.edu (L. Que).

<sup>\*</sup> Corresponding author.

(PET). PET is a non-invasive neuroimaging technique that indirectly measures neuronal activity or neurotransmitter release [20-21]. In nuclear medicine, detecting neurotransmitters are achieved by measuring the metabolic or molecular activity of an organ in three dimensions, after the intravenous injection of a radioactive tracer, usually based on an injected isotope with a short half-life, whose disintegration results in positron emission. However, the test requires complex operation, and the cost is very high, and the measurements must be carried out under stringently controlled conditions. In addition, sample handling, instrument operation, and data analysis are challenging and require trained personnel, rendering those tests unsuitable for straightforward routine tests. Other techniques such as electrochemical methods have been employed to measure and record the levels and status of these neurotransmitters [3,22-24]. Electrochemical detection relies on measuring electrical signals such as current, potential, or charge when the electrodes are exposed to chemical or biological samples [25]. The in vivo measurements of neurotransmitters in extracellular fluid have been demonstrated with carbon microelectrodes implanted into the brain of a rat [26]. The direct detection of neurotransmitters in the brain by this technique is very challenging given their very low concentrations, notwithstanding the presence of interfering compounds [27]. Electrochemical techniques are also widely used for in vitro measurements of neurotransmitters. Some popular techniques are DPV (Differential pulse voltammetry), SWV (Square wave voltammetry), and CV (Cyclic voltammetry) to obtain the transducing signals for neurotransmitters.

To improve the limit of detection (LOD) and sensitivity, the electrodes of the electrochemical sensors functionalized with various nanomaterials (2D hexagonal boron nitride, carbon dots, carbon nanofibers, nanoparticles, carbon nanotubes, nano Zn-Co on the metalorganic framework, graphene oxide, graphene quantum nanodots, and graphene nanocomposite, etc.) have been developed [24,28–32], which were used to detect dopamine or serotonin along with bio-interferents (ascorbic acid (AA), uric acid (UA), glucose, etc.). It showed that the LOD of these sensors is in a range of 10 to 650 nM for dopamine and 1 to 120 µM for serotonin, respectively [33]. Some of other recent work demonstrated the improved LOD and sensitivity of electrochemical sensors by fabricating micropillars/micro pyramids on the working electrode [34–35]. In the experiments, the working electrode was assembled inside a petri dish along with other commercial electrodes (reference and counter electrodes). The samples were then mixed with

electrolytes and added to the petri dish for the measurements in a static condition (i.e., no flowing fluid condition).

The body fluids continuously circulate in the body so that the essential substances can be transported to cells, while waste can be carried away [36]. However, few efforts were made to detect neurotransmitters under dynamic conditions (i.e., flowing fluid). Measurement under dynamic conditions is required to mimic the *in vivo* conditions [37–39]. One example is the *in vitro* dopamine detection from a mixture of cerebrospinal fluid and plasma of a mouse. This involves dynamic fluid movement on top of the electrochemical sensor in a microfluidic device [40]. Other examples include real-time monitoring of the concentrations of neurotransmitters in the culture media of the brain models which enables the quantitative analysis of their effect on brain models on chip [41–43].

Herein, we report an electrochemical sensing microchip (Fig. 1) enabled by nanostructured electrodes. The sensor has three gold electrodes anchored inside the detection chamber for monitoring neurotransmitters. To mitigate biofouling on the electrodes of the sensor [44], a microfilter zone is designed to filter out large biomolecules but allow neurotransmitters to easily diffuse to the sensors in the detection chamber. This microchip can detect dopamine and serotonin in both static and dynamic conditions. We also developed a modified microfluidic chip with an integrated cell-culture chamber to detect dopamine directly released from the N27-A dopaminergic neural cells, which are a widely used model for Parkinson's disease research [45–46].

#### 2. Materials and methods

#### 2.1. Chemicals and materials

The polystyrene nanosphere beads with different sizes (500 nm, 1000 nm, 3000 nm) were purchased from Fisher Scientific Inc. Triton X-100 and methanol were both purchased from Sigma-Aldrich Inc. Deionized (DI) water was obtained from a DI water purification system (Millipore, USA). The differentiation media (DM) included Dulbecco's modified Eagle's medium/Ham's/F² (DMEM/F-12, 1:1; Omega Scientific, Tarzana, CA), 2.5 mM L-glutamine,  $1 \times N2$  supplement (Gibco BRL, Gaithersburg, MD). Dopamine hydrochloride (DA), Serotonin (ST), Uric acid (UA), Ascorbic acid (AA), Glucose (GLC), L-dopa (LD), Tyrosine (TYRO), and Phenylalanine (PHE) were purchased from Sigma-Aldrich

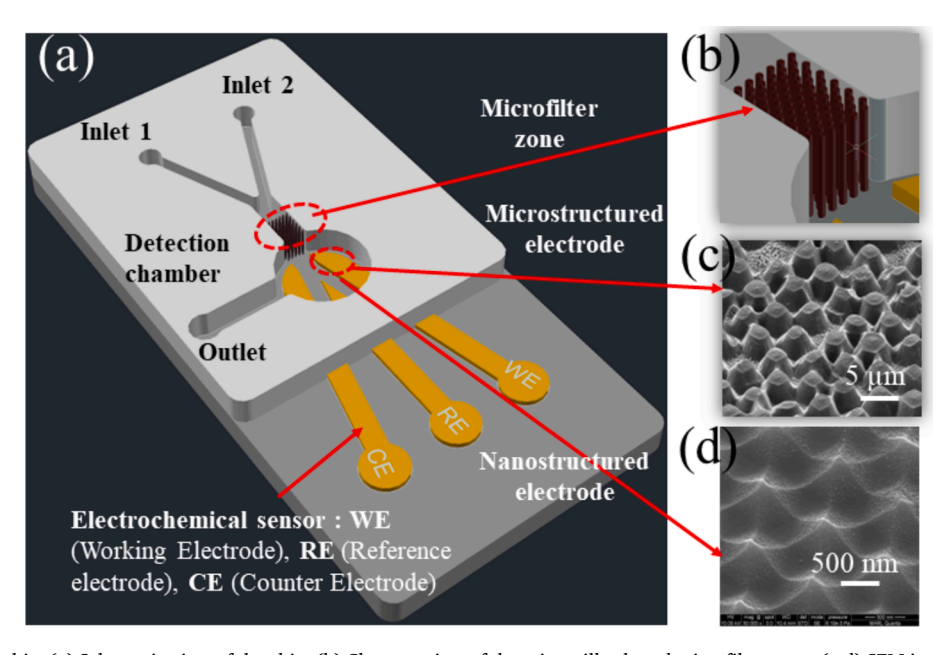


Fig. 1. Illustration of the chip: (a) Schematic view of the chip; (b) Close-up view of the micropillar-based microfilter zone; (c-d) SEM images of the silicon micro and nanopillar surface used as the template for fabricating PDMS micro or nanostructured electrodes.

(St. Louis, MO, USA). Silicon wafers were obtained from Ultrasil Corp. Chemicals for surface cleaning and treatment including Acetone, IPA, 98 % Sulfuric acid and 30 % Hydrogen peroxide were all obtained from Sigma-Aldrich Inc. Polydimethylsiloxane (PDMS) and its curing agent were purchased from Dow Corning (Midland, WI, USA). Positive photoresist AZ 40XT and AZ 326 MIF developer were purchased from MicroChemicals (Germany). N27-A rat dopaminergic neural cells were purchased from Millipore Corp. (Cat. # SCC196) (USA).

## 2.2. Fabrication and characterization of polymer electrochemical micro-

The main steps of the fabrication process of the chips are illustrated in Fig. 2. First, the micro/nanostructures were fabricated on silicon wafers. The micro/nanostructures fabrication procedure was adopted from our developed process [47-48]. Specifically, a monolayer of selfassembled polystyrene (PS) beads was formed on top of a cleaned silicon wafer using controlled flow and drying of the PS bead's solution (Fig. 2(a)). Then oxygen (O<sub>2</sub>) reactive ion etching (RIE) was performed to shrink the PS beads' diameters and increase the gaps between them (Fig. 2(b)). After that,  $O_2 + SF_6$  RIE was used to etch the silicon using the PS beads as the mask (Fig. 2(c)). Afterward, the PS beads were removed from the silicon surface using the sonication method (30 min) (Fig. 2 (d)). By adjusting the RIE time and different sizes of PS beads, silicon micro and nanostructures of different shapes and sizes can be fabricated [47–48]. The silicon micro/nanostructures were used as a mold for the next steps for electrode fabrication. Before using the micro/nanostructured silicon as a mold to transfer the micro/nanostructures to PDMS, it was silanized using trichloro silane to prevent the sticking of PDMS to the mold. The silanization process consisted of activating the surface of the mold using air plasma for 10 min and then incubating the mold with a silane reagent in the vacuum at room temperature for 10 h. After silanization, liquid PDMS (9:1, base: curing agent) was poured onto the silicon mold and kept in a vacuum for degassing for about 1 h. When all the bubbles were removed, the PDMS was left on a hotplate (at 45 °C) overnight for curing. After that, the PDMS with micro or nanostructures was peeled off from the silicon mold (Fig. 2(e)). Then the three-electrode pattern was transferred onto the PDMS surface using a shadow mask. In this step, Ti/Au (10 nm/120 nm) or Ti/Platinum (Pt) (10 nm/120 nm) was deposited using a magnetron sputtering process. As a result, the electrode surface was coated with Au or Pt to obtain an electrically conductive and chemically modified surface Fig. 2(f-g). Another layer of the PDMS microfluidic network was fabricated in a separate soft lithography process. Finally, these two PDMS layers were

bonded together after being treated with air plasma for 45 s, resulting in PDMS-based electrochemical sensing microchips. Two types of chips were fabricated using the above-mentioned process (Fig. 2(h)). In one type of chip, the electrodes were fabricated by coating a layer of Au on the PDMS micro-nanostructures, and in another type of chip, electrodes were fabricated by coating a layer of Pt. SEM images of the Au-coated nanostructures and the Pt-coated nanostructures on PDMS are shown in Fig. S1(A-B) in the Supplementary document. The chemical elements of the electrodes were analyzed using energy-dispersive X-ray spectroscopy (EDS) and are shown in Fig. S1(C-D) in the Supplementary document, the composition of the electrodes includes Au or Pt and PDMS, as expected.

Electrochemical impedance spectroscopy (EIS) of the Au & Pt electrodes fabricated on the nanostructured PDMS was measured from 1 Hz to 1 MHz frequency to evaluate the properties of the electrodes. More details can be found in Fig. S2 in the Supplementary document. Both electrodes manifest higher impedance in cell Differentiation Media (DM) than in 0.1 M PBS. In addition, the effects of scan rates on electrochemical sensing have been evaluated by cyclic voltammetry (CV) of ferri/ferro redox couples, DA, ST, and DA/ST mixture, which are given in detail in Fig. S3 in the Supplementary document. As expected, the oxidation and reduction peak currents increase linearly with scan rates in the range from 10 to 500 mV. The linear relationship indicates diffusion-controlled electrochemical detection using this sensor [35].

To assess the effectiveness of the electrode materials for electrochemical sensing, both electrochemical sensors fabricated on PDMS (PDMS-sensors) and electrochemical sensors fabricated on glass (glasssensors) have been used to detect 1 mM K<sub>3</sub>[Fe(CN)<sub>6</sub>]: K<sub>4</sub>[Fe(CN)<sub>6</sub>] 1:1 solution in 0.1 M PBS. As shown in Fig. S4 in the Supplementary document, the oxidation peak for both PDMS sensors and glass sensors was at 0.08 V. The oxidation peak currents were observed at 18  $\mu A$  for both types of sensors. The reduction peak was found at -0.1 V for the PDMS sensors and -0.05 V for the glass sensors. The reduction peak current for the PDMS sensors was  $-12~\mu A$ . The reduction peak current for the glass sensors was  $-16 \mu A$ . Although the reduction peak current did not coincide, the results indicate that the PDMS sensors can be used effectively as electrochemical sensing chip. Note that the main purpose of this research is to develop polymer nanostructured electrochemical sensors for potential implantable applications, requiring the sensor material to be biocompatible. Hence, only PDMS electrochemical sensors were used in the following experiments.

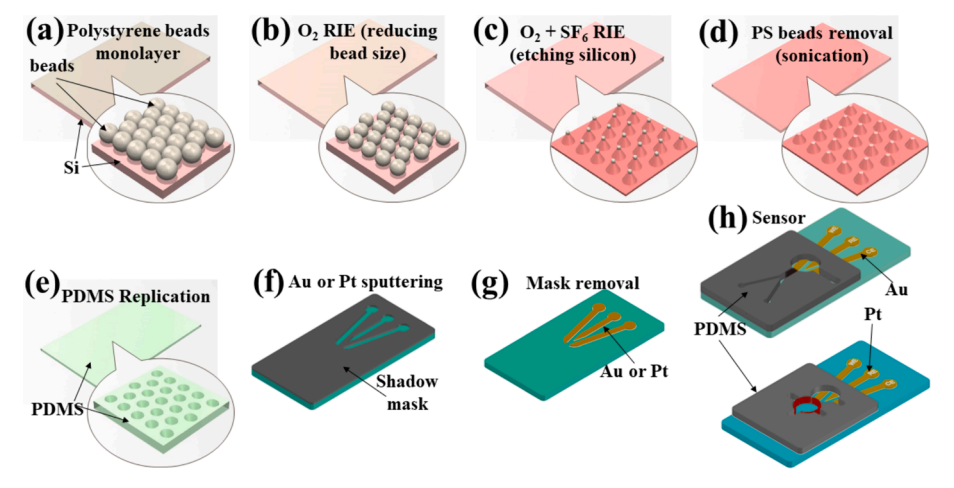


Fig. 2. Fabrication process flow: (a-d) Sketches of assembled PS beads on the silicon surface, followed by oxygen reactive ion etching (RIE), then  $O_2$  and  $SF_6$  RIE, resulting in silicon micro or nanopillars; (e) silicon micro or nanopillars are transferred to PDMS; (f-g) PDMS Au or Pt micro or nanostructured electrodes fabricated using a shadow mask and the sputtering method; (h) two type of chips are formed by bonding the PDMS microfluidic layer and the electrodes layer.

#### 2.3. Detection of dopamine and serotonin in static conditions

Dopamine and serotonin can be detected electrochemically upon oxidation on an electrode surface (Fig. 3a) [27]. Studies revealed that the neurotransmitter release occurred in the process known as exocytosis [49]. Upon external stimulation, Ca<sup>2+</sup> influx-induced neurotransmitters confined in vesicles dock and subsequently fuse with the plasma membrane, releasing the vesicular contents into the extracellular environment [49]. First, static condition measurements of the samples were taken to establish a baseline for dynamic condition measurements. In these experiments, the samples were added to the chip without continuous flow. Cyclic voltammetry (CV) and square wave voltammetry (SWV) were used to electrochemically detect dopamine and serotonin with the following parameters for CV: range, -0.4-+0.6 V; scan rate, 100 mV/s; incremental potential, 0.002 V. The following parameters were used for SWV: range, -0.4-+0.6 V; Step, 0.005 V; modulation amplitude, 0.005 V; frequency, 8 Hz; duration, 27.25 s.

#### 2.4. Detection of dopamine and serotonin in dynamic conditions

In dynamic conditions, the electrochemical measurements were taken when the samples flowed through the chip through its inlets and outlets. During the experiments, the flow rate of the samples was controlled by a programmable injection pump (Harvard Apparatus, Inc.) and included flow rates of 1, 2.5, and 5  $\mu$ l/min. Reading of the electrochemical sensor was taken every three minutes up to fifteen minutes. Square wave voltammetry (SWV) was performed for dynamic condition measurements. After each measurement, the electrodes were washed three times using fresh PBS solution to move away the analyte remaining from the previous measurements to regenerate the sensor (Fig. S5 in the Supplementary document). Each measurement was performed thrice.

## 2.5. Detection of dopamine released directly from N27-A cells

N27-A cells exhibit higher sensitivity to neurotoxins as compared to parental N27 cells [50], and release dopamine under both basal and depolarization conditions. To demonstrate the real-time monitoring of the dopamine released from N27-A cells, a modified microchip with an integrated cell chamber adjacent to the detection chamber is designed and fabricated, which will be described in detail in Section 3.3.

## 3. Results and discussion

# 3.1. Effects of micro-nanostructures on working electrodes of electrochemical sensors

To assess the effects of the working electrode surface on the

transducing signals, cyclic voltammetry of potassium ferrocyanide/potassium ferricyanide mixture, a widely used test chemical for evaluating the performance of electrochemical sensors [35,51], was performed for three different sensors with plain, micro-structured, and nanostructured electrodes, respectively. The samples were prepared using the mixture (1:1 ratio) of 1 mM K<sub>4</sub>Fe(CN)<sub>6</sub>/K<sub>3</sub>Fe(CN)<sub>6</sub> in 0.1 M phosphate-buffered saline (PBS) solution. One representative photo of a fabricated chip with micropillar electrodes and the diagrams of the electrochemical reaction of dopamine and serotonin are shown in Fig. 3 (a). The cyclic voltammograms for three sensors with different electrode surface conditions are shown in Fig. 3(b). It has been found that with the plain electrode surface, the output peak current was 1.0 mA. For the micro-pillar electrode surface, the output peak current increased slightly to 1.2 mA. For the nano-pillar electrode surface, the output peak current was 2.0 mA, which is two times the output current observed in the plain electrode surface. This increase is likely due to the enhanced surface area of the nanostructured electrodes in comparison with those of microstructured electrodes and plain electrodes [34]. In the following experiments, sensors with nanostructured electrodes were used. The samples of dopamine and serotonin were prepared by using a series of ratios in 0.1 M PBS solution and differentiation media (DM), respectively.

## 3.2. Measurement of DA and serotonin (ST) in samples under static conditions

#### 3.2.1. DA and ST measurements separately

Electrochemical measurements of DA and ST were first taken in static conditions. SWV method was chosen over the CV method to avoid the effect of the non-faradic currents which cause the unclear oxidation peak at lower concentrations. The measurements were taken in a wide range of concentrations from 1 nM to 500  $\mu$ M. The measurements of DA and ST for these concentrations were displayed in Fig. 4(a-c) and (d-f). DA peak current was observed at a potential of  $\sim 0.007 \text{ V}$  and ST peak was observed at a potential of  $\sim 0.1~\text{V}.$  It was also observed as shown in Fig. 4(c) and (f) that the peak current responses have a linear relationship with the DA and ST concentrations, respectively. Additional plots of peak current response for DA and ST of higher concentrations are given in Fig. S6 in the Supplementary document. The sensitivity for DA was found 0.05  $\mu A/\mu M$  and for ST was found 0.04  $\mu A/\mu M$ . The limit of detection (LOD) of the sensor was determined by the peak current, which is greater than the average current at zero concentration of DA or  $ST + 3\sigma$  ( $\sigma$  is the standard deviation of peak current from zero concentration) [52]. The LOD for DA was found to be  $\sim 120$  nM and the LOD for ST it was found to be  $\sim$  140 nM. It should be noted that the sizes of the electrodes for the sensors in the microchip are  $\sim 3.5$  mm (length) × 1.5 mm (width), thus the sensing surfaces exposed to chemicals are

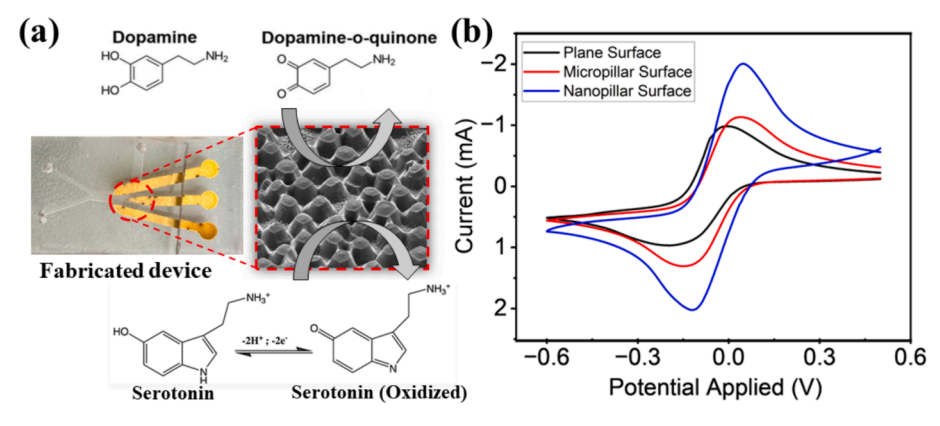


Fig. 3. Effect of micro-nanostructured working electrode: (a) photo of a fabricated PDMS chip, and illustration of electrochemical oxidation of dopamine and serotonin, (b) Flat, micro-structured, and nano-structured Au electrode surface oxidation current comparison. 1 mM  $K_4$  Fe (CN) $_6/K_3$  Fe (CN) $_6$  (1:1 ratio) in 0.1 M PBS solution was used for calibration and surface effect comparison of the sensors.

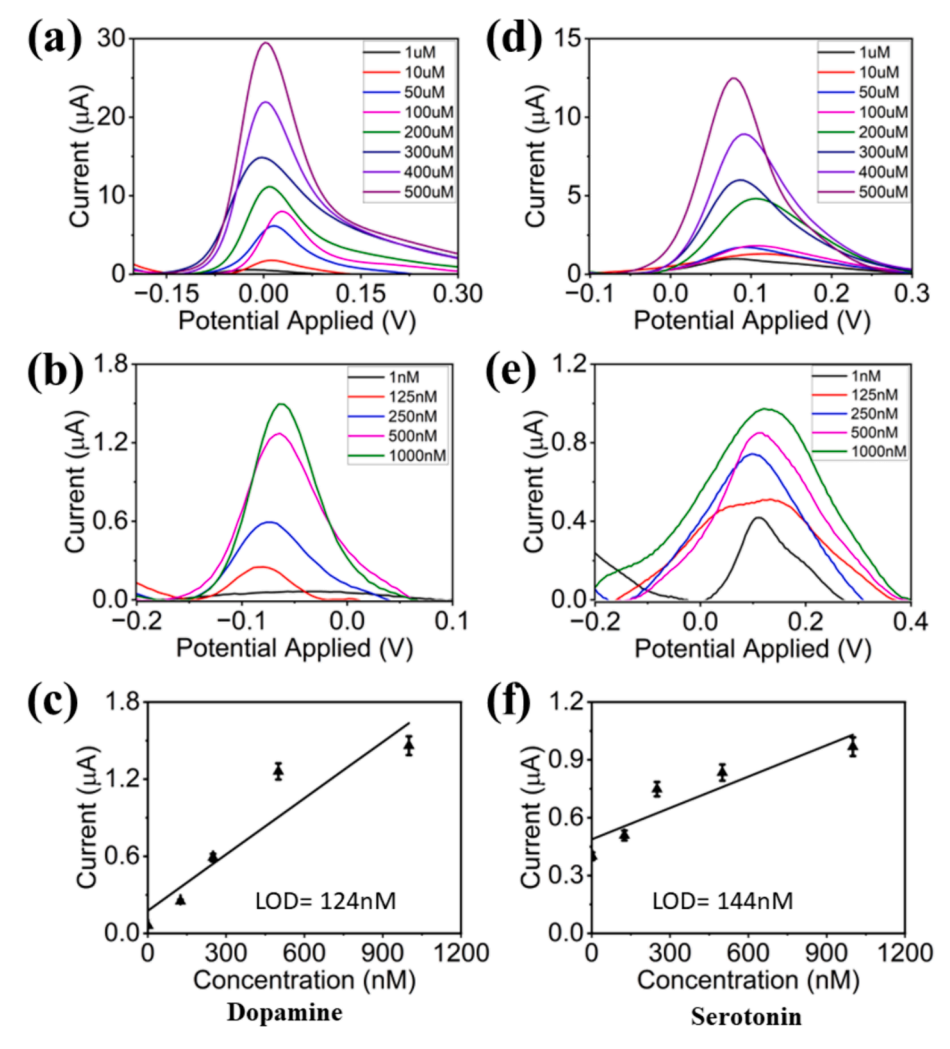


Fig. 4. Measurement of DA and ST in PBS buffer: (a-c) Dopamine detection using SWV method (DA concentrations from 1 nM to 500  $\mu$ M); (d-f) Serotonin detection using SWV method (ST concentrations from 1 nM to 500  $\mu$ M).

much smaller than those of commercially macroscale electrodes of cylinder shape with a typical size of 32 mm (length)  $\times$  0.5 mm (radius) (CHI-102, platinum working electrode, CH Instruments, Inc.). In addition, in the microchip, the electrodes are fabricated on the planar surface, and the exposure surface to chemicals is, therefore, further limited compared to that of macro electrodes, whose cylinder shape allows greatly increased surface exposure to chemicals. Moreover, the volume of the sample used for this experiment was only 40–60  $\mu l$  per measurement which is very small compared to the commercial macro electrode volume. All these factors contribute to the LOD of the electrodesbased electrochemical sensors. It is anticipated that the LOD can be potentially enhanced by fabricating 3D electrodes on chips and optimizing the nanostructures on the electrodes.

#### 3.2.2. Measurements of DA and ST mixed samples

The samples were prepared by mixing DA and ST of the same concentration. Specifically, the mixed samples with DA and ST concentrations range from 0.5  $\mu$ M to 250  $\mu$ M in both PBS buffer and DM. The measured results of the samples in PBS buffer are shown in Fig. 5(a), while the measured results of the samples in DM are given in Fig. 5(b).

For measurements of samples in PBS solution, the presence of ST in the mixture does affect the DA peak current. It was observed that it was  $\sim 2 \times$  times less (approx.) peak current compared to ST peak current for the same concentration. ST peak current was observed at 1.1  $\mu A$  peak current for 0.5  $\mu M$  concentration following a linear relationship up to

 $10.1\mu A$  current for  $250~\mu M$  concentration. In contrast, DA peak current was observed at  $0.1~\mu A$  peak current for  $0.5~\mu M$  concentration following a linear relationship up to 4.9  $\mu A$  current for  $250~\mu M$  concentration. A similar trend was also observed for measurements of samples in DM. It was observed that in DM, the DA peak current was half of the ST peak current. ST peak current followed a linear relationship measuring from 0.5 to  $250~\mu M$  concentration. DA peak current also follows a linear relationship measuring from 0.5 to  $250~\mu M$  concentration. For both measurements, the peak currents for DA and ST appear, indicating the sensor was able to distinguish DA and ST in mixed samples.

It has been observed that the current peaks for DA and ST slightly shift to higher potentials for samples in PBS buffer and DM. Specifically, for DA, the oxidation potential shifted from  $\sim 0.04$  V to  $\sim 0.08$  V, and for ST, from  $\sim 0.20$  V to  $\sim 0.27$  V when the electrolyte fluid was changed from PBS buffer to DM. Another observed deviation is the magnitudes of the peak currents for both DA and ST, which were almost reduced to half for the samples in DM in comparison with those in PBS buffer since the electrical conductivity is higher for PBS buffer (10.6 S/m) [53] than that of DM (1.515 S/m) [54].

## 3.2.3. Evaluation of the sensor's specificity

The specificity assessment was performed by mixing DA and ST with interfering molecules, which coexist not only in the extra-cellular central nervous system but also in different body fluids [55]. The oxidation potentials of DA and ST could overlap with those of other molecules and

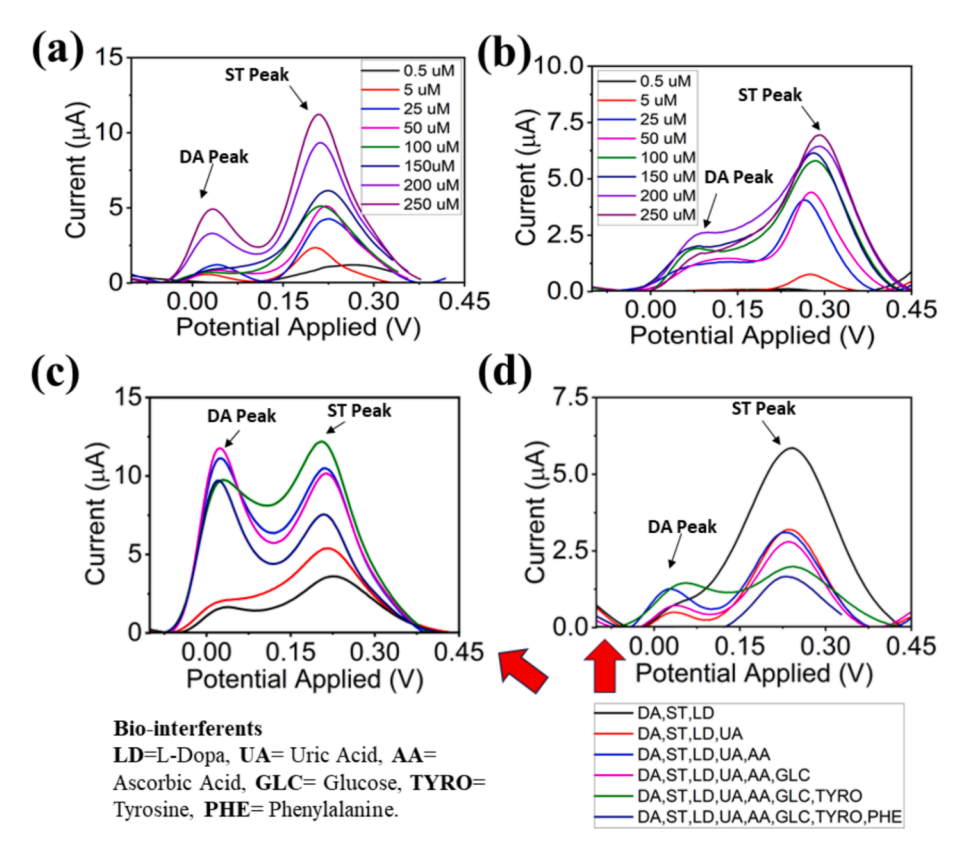


Fig. 5. Detection of DA and ST in mixed samples under static conditions. (a) Detection of DA and ST mixtures in PBS buffer; (b) detection of DA and ST mixtures in DM; (c) selectivity measurement in PBS buffer; (d) selectivity measurement in DM. Five chips were used for the experiments. For the same chip, at least three measurements were taken.

thus produce a false positive signal. Specifically, the samples were prepared by mixing 250 µM DA, ST, Uric acid (UA), Ascorbic acid (AA), L-dopa (LD), Tyrosine (TYRO), Phenylalanine (PHE), and 1 mM Glucose (GLC).

The interfering molecules were added one by one, starting with LD, into the samples, while keeping the DA and ST mixture concentration constant. Electrochemical measurements were carried out for the samples in both PBS buffer and DM. The results are shown in Fig. 5(c) and 5 (d). GLC was selected as an interfering molecule due to its presence in the media. However, GLC does not undergo an electrochemical reaction directly in a solution. Hence, a negligible effect is expected in the DA and ST peaks in the presence of GLC in the solution. It is verified by comparing the peak magnitude for the mixed sample (DA, ST, LD, UA, and AA) and that for the mixed sample (DA, ST, LD, UA, AA, and GLC). DA and ST peak currents were observed almost in the same magnitude for samples in PBS and DM. LD has an oxidation potential of 0.22 V and falls within the range of DA and ST oxidation window [56]. So, the peak currents of DA and ST are expected to be impacted by the presence of LD in the mixture. DA and ST peak currents were observed as lowest for the mixed sample (DA, ST, and LD) compared to other mixed samples in PBS solution. DA peak is almost invisible for the mixed sample (DA, ST, and LD) in DM. However, the ST peak was the highest in magnitude as it was influenced by the presence of LD in the mixed sample in DM which was reduced in the subsequent measurements. UA, AA, PHE, and TYRO are also electrochemically active molecules with oxidation potentials of 0.6 V, 0.47 V, 0.5 V, and 0.65 V to standard reference electrodes, respectively [57-60]. A negligible effect was expected from these interferents as their oxidation potential falls outside the experimental potential window (-0.1 V to 0.45 V) of DA and ST. However, their presence significantly affected the DA and ST peaks of samples in PBS, but did not significantly affect those peaks of samples in DM. One approach to further mitigate or even eliminate the interference from these interfering molecules is to use ion-separation layers such as Nafion membranes, which can prevent those molecules from reaching sensors, but only allow DA or ST to reach sensors [35].

It was observed that despite the presence of different interfering molecules, both DA and ST peaks were still observed clearly, indicating very good specificity of the sensors. For the samples in the PBS buffer, the DA peaks were observed at  $\sim 0.04$  V and ST peaks at  $\sim 0.20$  V, similar to those of the samples without interfering molecules. For the samples in DM, the DA peaks were observed at  $\sim 0.08$  V and ST peaks at  $\sim 0.27$  V, again similar to those of the samples without interfering molecules. In addition, it was also observed that the presence of interfering molecules in the samples reduced the magnitudes of the peak currents for both DA and ST.

## 3.3. Measurement of DA and ST in samples under dynamic conditions

## 3.3.1. Detection of DA and ST mixed samples

Integration of *in vivo* microdialysis with selective electrochemical detection to form online analytical systems for continuously monitoring neurochemicals has been proven to be particularly useful and readily amenable for probing brain chemistry [46]. As an example, for measurements of samples under dynamic conditions, Fig. 6(a) shows 15 min of continuous monitoring output for the concentration of 200  $\mu M$ . It was observed that the DA peak was found to be at 0.1 V and the ST peak was found to be at 0.3 V, which moved towards the right compared to the results we got in the static measurements (Fig. 5). Because of the dynamic condition, the reference changed for the electrochemical measurements. Moreover, the output current decreased significantly (five times lower than the static condition) as the detected molecules moved away from the sensor surface more quickly by the continuously flowing solution. Fig. 6(b) shows the detection of DA and ST in PBS buffer for concentrations ranging from 50 to 250  $\mu M$ . The peak currents are

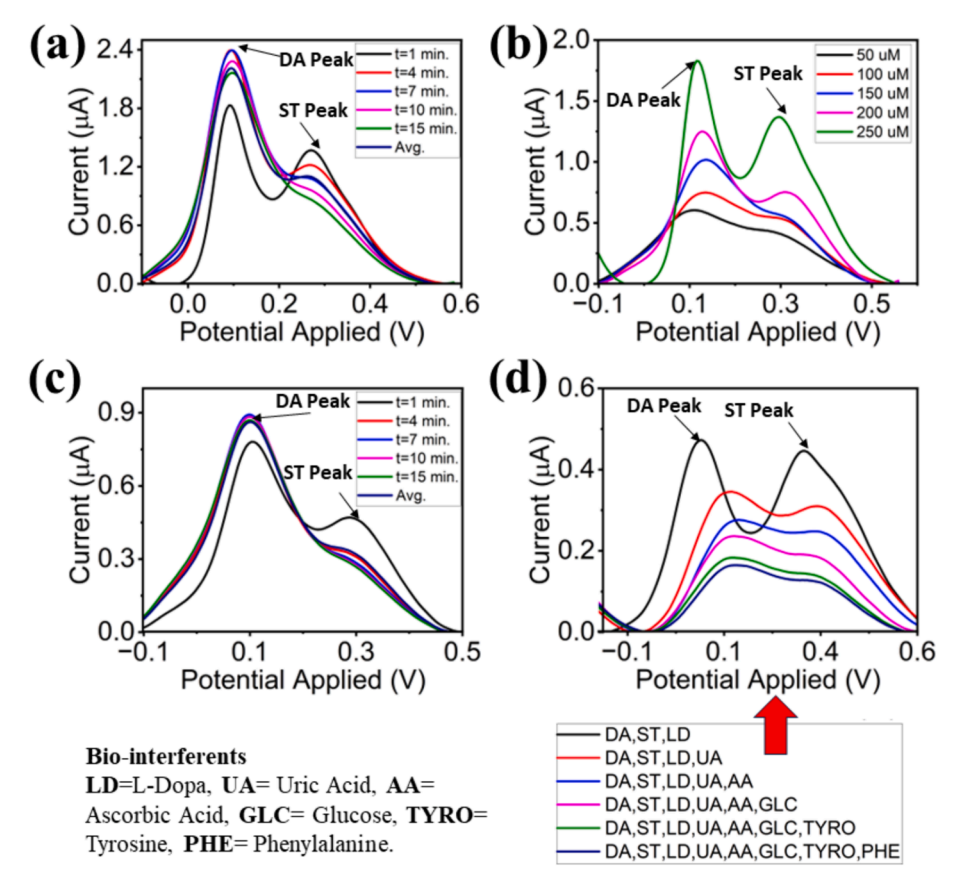


Fig. 6. Detection of DA and ST in mixed samples under dynamic conditions: (a) Detection at different timepoints for a concentration of 200  $\mu$ M of DA and ST; (b) detection of DA and ST with different concentrations in PBS buffer; (c) selectivity measurement at different timepoints; (d) selectivity measurement in PBS buffer. Five chips were used for the experiments. For the same chip, at least three measurements were taken.

obtained by averaging the measured peak currents from 15-minute continuous monitoring for each concentration. For measurements in dynamic conditions, the presence of ST in the mixture does affect the DA peak current as in the static measurements. Unlike the static condition, DA peak currents were observed to be approximately  $1.3\times$  higher than ST peak currents. ST peak current was observed at  $0.4~\mu A$  for  $50~\mu M$  concentration following a linear relationship up to  $1.35~\mu A$  current for  $250~\mu M$  concentration. DA peak current was observed at  $0.5~\mu A$  for  $50~\mu M$  concentration following a linear relationship up to  $1.8~\mu A$  for  $250~\mu M$  concentration. Overall, ST peak current decreased significantly (from  $10.1~\mu A$  to  $1.35~\mu A$ ) and DA peak current decreased significantly (from  $4.9~\mu A$  to  $1.8~\mu A$ ) for  $250~\mu M$  concentration in dynamic conditions.

## 3.3.2. Evaluation of specificity of the sensors

The selectivity of the sensors was also assessed for samples in dynamic conditions in a PBS buffer. Similar to the static results, DA and ST can be detected despite the presence of bio-interfering molecules (LD, UA, AA, GLC, TYRO, PHE) in the samples. Fig. 6(c) shows 15 min of continuous monitoring output for the concentration of 200 µM. Selectivity test results are presented in Fig. 6(d). The peak currents are obtained by averaging the measured peak currents from the 15 min of continuous monitoring for each concentration. DA peak was observed to be at  $\sim 0.04$  V and ST peak was observed to be at  $\sim 0.3$  V for the DA, ST, and LD mixture. After adding Uric Acid (UA) to the mixture, the peaks were shifted to  $\sim 0.1$  V for DA and  $\sim 0.4$  V for ST. These peak positions remained unchanged for the rest of the interferents, which is distinct compared to each other, indicating very good specificity of the sensors. However, it was observed that the presence of interfering molecules caused a decreased output current compared to the static measurement due to the dynamic condition. DA peak current was 0.5  $\mu A$  and ST peak current was 0.42  $\mu A$  for the mixture (DA, ST, and LD). Both DA peak current and ST peak current decreased linearly in specificity measurements performed in dynamic conditions. In addition, both peak currents were decreased linearly for adding each of the bio-interferents to the mixture. So, the introduction of each interferent in the mixture negatively affected the DA and ST peak currents. Adding more molecules into the mixture makes it harder for DA and ST molecules to diffuse to the sensor surface due to a crowded environment in dynamic measurements.

## 3.4. Real-time detection of dopamine released directly from N27-A cells

The layout of the modified chip is illustrated in Fig. 7(a) and a photo of a fabricated chip is shown in Fig. 7 (b). This chip consists of two chambers (C1 and C2) adjacent to each other and separated by a microfilter zone, which consists of arrayed micropillars. N27-A cells were plated in the cell-culture chamber (C<sub>1</sub>) through the inlet (I<sub>1</sub>) using a syringe. N-27A cells were trapped inside  $C_1$  by a surrounded ring of the microfilter while excess culture media could exit the  $C_1$  through the outlets (O1 or O2). Filter-sterilized KCl solution for cell excitation is supplied to the  $C_1$  through the inlet (I<sub>2</sub>). Three electrochemical sensor electrodes were fabricated inside the detection chamber (C2). The dopamine released from N27-A cells can diffuse into  $C_2$  from  $C_1$  and thus can be detected by the electrochemical sensor. The chip was fabricated using the process flow described in Fig. 2. The electrodes were fabricated using platinum (Pt) since the gold (Au) electrodes might be oxidized by KCl solutions, resulting in degraded performance and shortened lifetime of the sensor, especially for the miniaturized Au electrodes in the microchip [61]. In addition, it has been found that no peak currents in a potential range (-0.3 V to 0.3 V), which is relevant to the dopamine's oxidation potential for Pt electrode [62], can be observed for KCl

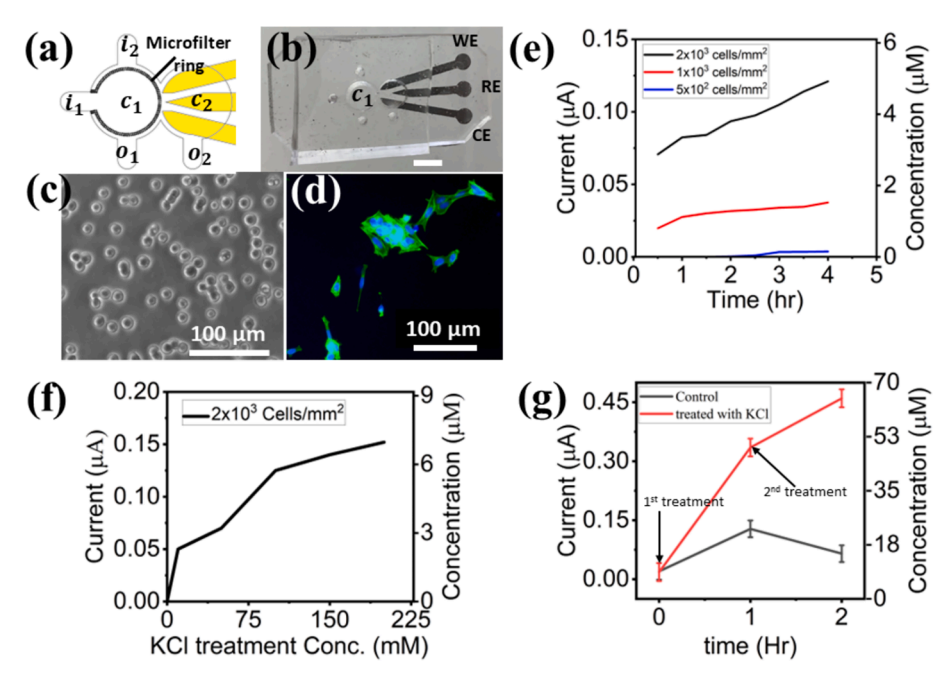


Fig. 7. Monitoring of dopamine released from N27-A cells: (a) Sketch of chip with a cell-culture chamber surrounded by a ring-shaped microfilter and detection chamber; (b) photo of a fabricated chip. Scale bar is 5 mm; (c) representative micrograph showing N27-A cells cultured in the cell-culture chamber on chip; and (d) N27-A cell images after being fixed and stained for phalloidin (green) and nucleus (blue) in the cell-culture chamber on chip; (e) measured peak current responses of  $5 \times 10^2$  cells/mm<sup>2</sup>,  $1 \times 10^3$  cells/mm<sup>2</sup>, and  $2 \times 10^3$  cells/mm<sup>2</sup> N-27A cells during 100 mM KCl treatment for four hours; (f) measured peak current responses (i.e., dopamine release) after two hours of 0, 10, 50,100, 150, and 200 mM KCl treatment; (g) measured dopamine release after repetitive (twice) KCl excitation of  $5 \times 10^5$  cells/mm<sup>2</sup> N27-A cells. (For interpretation of the references to colour in this figure legend, the reader is referred to the web version of this article.)

solutions using Pt-electrodes (Fig. S7 in Supplementary document), indicating KCl does not interfere with the DA readings. In the experiments, N27-A rat dopaminergic neural cells were revived using the supplier guidelines. Specifically, 10 % FBS and 1 % Penicillin-Streptomycin in RPMI-1640 1X media were used to culture and maintain the cells. N27-A cells were seeded and incubated for 10 h inside the cell-culture chamber  $C_1$  on the chip, where cells were grown in aseptic conditions without any chance of possible contamination. Then KCl solutions were added to  $C_1$ . Measurements were taken while the cells were in incubation. Representative optical micrographs and fluorescence images of the cells cultured in  $C_1$  are shown in Fig. 7(c-d).

The DA peak current was increased from 0.07  $\mu A$  to 0.12  $\mu A$  after four hours of continuous treatment with 100 mM KCl for  $2\times 10^3$  cells/mm² as shown illustrated in Fig. 7(e). Minimal dopamine release (e.g., the magnitude of DA peak current) was observed for  $5\times 10^2$  cells/mm² compared to  $1\times 10^3$  cells/mm² and  $2\times 10^3$  cells/mm². To further investigate the effect of KCl treatment concentration,  $2\times 10^3$  cells/mm² were treated with KCl with a series of concentrations of 0, 10, 50,100, 150, and 200 mM. As shown in Fig. 7(f), the peak current increases from 0.12  $\mu A$  to 0.16  $\mu A$  by increasing KCl concentration from 100 mM to 200 mM after two hours of treatment.

To assess the effect of repetitive KCl excitations, the samples with 5  $\times$   $10^5$  cells/mm  $^2$  N27-A cells were cultured in the cell-culture chambers on chips and excited with KCl twice in two hours. First, the measurements of the samples on chips were taken before any KCl excitations. Afterwards, 100 mM KCl was applied. Then electrochemical measurements were taken one hour later. The media in the cell-culture chamber with cells were  $\it washed$  with PBS, and fresh media were added to the chips, followed by the second KCl treatment. Another hour later, electrochemical measurements were carried out again. The measured results are shown in Fig. 7(g). After the first KCl treatment, 0.32  $\mu A$  peak current was observed, and after 2nd KCl treatment 0.45  $\mu A$  peak current was observed, corresponding to 37.05  $\mu M$  dopamine and 69.55  $\mu M$  dopamine, respectively, which were calculated based on the calibration curve of the sensor for dopamine. For control (i.e., without any KCl

treatment), the highest peak current after 1 hr was observed at 0.12  $\mu A$ , which corresponds to 4.24  $\mu M$  dopamine, then dropped. This indicates the presence of dopamine in the control sample even without any KCl treatment. The released dopamine from N27-A cells is significantly lower than after stimulation, which is consistent with previous publications [46].

## 4. Conclusions

In summary, microchips with integrated nanostructured-electrodes electrochemical sensors have been developed for detecting dopamine and serotonin in PBS buffer and DM under both static conditions and dynamic conditions. The LOD of the chips was found to be  $\sim 120 \text{ nM}$  for DA and 140 nM for ST, respectively. It has been demonstrated that the chips have very good specificity, which can distinguish DA and ST simultaneously from other bio-interfering molecules such as ascorbic acid, uric acid, glucose, tyrosine, and phenylalanine in mixed samples, again under both static conditions and dynamic conditions. Finally, the real-time monitoring of dopamine released from N27-A cells has been demonstrated, particularly when N27-A cells were under 100 mM KCl stimulation. Given the biocompatibility of the chip, since all the materials of the chip are biocompatible PDMS, this chip can be potentially used for achieving ex vivo DA or ST detection in brain tissues. More importantly, it could be made implantable for in vivo monitoring of DA or ST in animal subjects or even humans, thereby providing a technical toolset to gain insightful information on neurotransmitters related to various neurological and psychiatric diseases.

## CRediT authorship contribution statement

Md Fazlay Rubby: Writing – review & editing, Writing – original draft, Methodology, Investigation, Formal analysis, Data curation. Catharine Fonder: Writing – review & editing, Investigation. Sajid Uchayash: Writing – review & editing, Investigation, Formal analysis. Shafayet Ahmed Siddiqui: Writing – review & editing, Investigation,

Formal analysis, Data curation. Ian Schneider: Writing – review & editing, Supervision, Methodology. Donald S. Sakaguchi: Writing – review & editing, Supervision, Investigation. Long Que: Writing – review & editing, Writing – original draft, Supervision, Methodology, Investigation, Funding acquisition, Formal analysis, Conceptualization.

## Declaration of competing interest

The authors declare that they have no known competing financial interests or personal relationships that could have appeared to influence the work reported in this paper.

#### Data availability

Data will be made available on request.

## Acknowledgments

We would like to thank the technical staff at Microelectronics Research Center (MRC) and Dr. Warren Straszheim at MARL, Iowa State University for their technical support. This research was funded in part by the Exploratory Research Program at Iowa State University and NSF CMMI 2031826.

## Appendix A. Supplementary data

Supplementary data to this article can be found online at https://doi.org/10.1016/j.microc.2024.111159.

#### References

- [1] Y. Qiu, Y. Peng, J. Wang, Immunoregulatory role of neurotransmitters, Adv. Neuroimmunol. 6 (3) (1996) 223–231.
- [2] N. Chauhan, S. Soni, P. Agrawal, Y.P.S. Balhara, U. Jain, Recent advancement in nanosensors for neurotransmitters detection: Present and future perspective, Process Biochem. 91 (2020) 241–259.
- [3] Z. Tavakolian-Ardakani, O. Hosu, C. Cristea, M. Mazloum-Ardakani, G. Marrazza, Latest trends in electrochemical sensors for neurotransmitters: A review, Sensors 19 (9) (2019) 2037.
- [4] A.V. Terry Jr, J.J. Buccafusco, C. Wilson, Cognitive dysfunction in neuropsychiatric disorders: selected serotonin receptor subtypes as therapeutic targets, Behav. Brain Res. 195 (1) (2008) 30–38.
- [5] H. Braak, K. Del Tredici, U. Rüb, R.A. De Vos, E.N.J. Steur, E. Braak, Staging of brain pathology related to sporadic Parkinson's disease, Neurobiol. Aging 24 (2) (2003) 197–211.
- [6] A. Sharma, M.A. Smith, D.F. Muresanu, P.K. Dey, H.S. Sharma, 5-Hydroxytryptophan: a precursor of serotonin influences regional blood-brain barrier breakdown, cerebral blood flow, brain edema formation, and neuropathology, Int. Rev. Neurobiol. 146 (2019) 1–44.
- [7] C. Kraus, E. Castrén, S. Kasper, R. Lanzenberger, Serotonin and neuroplasticity-links between molecular, functional and structural pathophysiology in depression, Neurosci. Biobehav. Rev. 77 (2017) 317–326.
- [8] D. Švob Štrac, N. Pivac, D. Mück-Seler, The serotonergic system and cognitive function, Transl. Neurosci. 7 (1) (2016) 35–49.
- [9] P. Olgiati, E. Bajo, M. Bigelli, D. De Ronchi, A. Serretti, Should pharmacogenetics be incorporated in major depression treatment? Economic evaluation in high-and middle-income European countries, Progr. Neuro-Psychopharmacol. Biolog. Psychiatry 36 (1) (2012) 147–154.
- [10] A. Serretti, P. Olgiati, E. Bajo, M. Bigelli, D. De Ronchi, A model to incorporate genetic testing (5-HTTLPR) in pharmacological treatment of major depressive disorders, World J. Biol. Psychiatry 12 (7) (2011) 501–515.
- [11] M. Biondi, A. Agostoni, B. Marasini, Serotonin levels in hypertension, J. Hypertens. Suppl.: Off. J. Int. Soc. Hypertens. 4 (1) (1986) S39–S41.
- [12] Moskwa, A.; Boznańska, P., Role of serotonin in the pathophysiology of the irritable bowel syndrome. Wiadomosci Lekarskie (Warsaw, Poland: 1960) 2007, 60 (7-8), 371-376.
- [13] S.J. Finnema, M. Scheinin, M. Shahid, J. Lehto, E. Borroni, B. Bang-Andersen, J. Sallinen, E. Wong, L. Farde, C. Halldin, Application of cross-species PET imaging to assess neurotransmitter release in brain, Psychopharmacology 232 (2015) 4129–4157.
- [14] F. Wu, P. Yu, L. Mao, Analytical and quantitative in vivo monitoring of brain neurochemistry by electrochemical and imaging approaches, ACS Omega 3 (10) (2018) 13267–13274.
- [15] E.S. Mitchell, J.F. Neumaier, 5-HT6 receptors: a novel target for cognitive enhancement, Pharmacol. Ther. 108 (3) (2005) 320–333.

- [16] A. Gröger, R. Kolb, R. Schäfer, U. Klose, Dopamine reduction in the substantia nigra of Parkinson's disease patients confirmed by in vivo magnetic resonance spectroscopic imaging, PLoS One 9 (1) (2014) e84081.
- [17] D. Chatterjee, R. Gerlai, High precision liquid chromatography analysis of dopaminergic and serotoninergic responses to acute alcohol exposure in zebrafish, Behav. Brain Res. 200 (1) (2009) 208–213.
- [18] T. Yoshitake, S. Yoshitake, K. Fujino, H. Nohta, M. Yamaguchi, J. Kehr, High-sensitive liquid chromatographic method for determination of neuronal release of serotonin, noradrenaline and dopamine monitored by microdialysis in the rat prefrontal cortex, J. Neurosci. Methods 140 (1–2) (2004) 163–168.
- [19] T. Yoshitake, J. Kehr, S. Yoshitake, K. Fujino, H. Nohta, M. Yamaguchi, Determination of serotonin, noradrenaline, dopamine and their metabolites in rat brain extracts and microdialysis samples by column liquid chromatography with fluorescence detection following derivatization with benzylamine and 1, 2diphenylethylenediamine, J. Chromatogr. B 807 (2) (2004) 177–183.
- [20] Y. Petibon, N.M. Alpert, J. Ouyang, D.A. Pizzagalli, C. Cusin, M. Fava, G. El Fakhri, M.D. Normandin, PET imaging of neurotransmission using direct parametric reconstruction, Neuroimage 221 (2020) 117154.
- [21] R.N. Lippert, A.L. Cremer, S. Edwin Thanarajah, C. Korn, T. Jahans-Price, L. M. Burgeno, M. Tittgemeyer, J.C. Brüning, M.E. Walton, H. Backes, Time-dependent assessment of stimulus-evoked regional dopamine release, Nat. Commun. 10 (1) (2019) 336.
- [22] K.E. Dunham, B.J. Venton, Electrochemical and biosensor techniques to monitor neurotransmitter changes with depression, Anal. Bioanal. Chem. (2024) 1–18.
- [23] S.E. Elugoke, P.S. Ganesh, S.Y. Kim, E.E. Ebenso, Common Transition Metal Oxide Nanomaterials in Electrochemical Sensors for the Diagnosis of Monoamine Neurotransmitter-related Disorders, ChemElectroChem (2024) e202300578.
- [24] V.A. Tran, G.N. Vo, V.D. Doan, N.C. Thanh, T. Dai Lam, Modification sub-nano Zn-Co Metal-Organic framework for electrochemical detection of neurotransmitter, Microchem. J. 197 (2024) 109852.
- [25] S. Banerjee, S. McCracken, M.F. Hossain, G. Slaughter, Electrochemical detection of neurotransmitters, Biosensors 10 (8) (2020) 101.
- [26] P.T. Kissinger, J.B. Hart, R.N. Adams, Voltammetry in brain tissue—a new neurophysiological measurement, Brain Res. 55 (1) (1973) 209–213.
- [27] R.N. Adams, Probing brain chemistry with electroanalytical techniques, Anal. Chem. 48 (14) (1976) 1126A–A1138.
- [28] C. Liu, X. Lin, J. Liao, M. Yang, M. Jiang, Y. Huang, Z. Du, L. Chen, S. Fan, Q. Huang, Carbon dots-based dopamine sensors: Recent advances and challenges, Chin. Chem. Lett. 109598 (2024).
- [29] C. Côrtes, J.C. Mantilla, S.W. da Silva, G.A. Camara, M.J. Giz, A sensitive and selective platinum-based electrochemical sensor for detection of neurotransmitters: Design and proof of concept, Microchem. J. 193 (2023) 109017.
- [30] Y. Zhang, L. Zhang, C. Li, J. Han, W. Huang, J. Zhou, Y. Yang, Hydrophilic antifouling 3D porous MXene/holey graphene nanocomposites for electrochemical determination of dopamine, Microchem. J. 181 (2022) 107713.
- [31] H. Guan, B. Liu, D. Gong, B. Peng, B. Han, N. Zhang, Direct electrochemical enhanced detection of dopamine based on peroxidase-like activity of Fe3O4@ Au composite nanoparticles, Microchem. J. 164 (2021) 105943.
- [32] Q. Huang, X. Lin, L. Tong, Q.-X. Tong, Graphene quantum dots/multiwalled carbon nanotubes composite-based electrochemical sensor for detecting dopamine release from living cells, ACS Sustain. Chem. Eng. 8 (3) (2020) 1644–1650.
- [33] S. Durairaj, B. Sidhureddy, J. Cirone, A. Chen, Nanomaterials-based electrochemical sensors for in vitro and in vivo analyses of neurotransmitters, Appl. Sci. 8 (9) (2018) 1504.
- [34] M. Senel, M. Dervisevic, S. Alhassen, A. Alachkar, N.H. Voelcker, Electrochemical micropyramid array-based sensor for in situ monitoring of dopamine released from neuroblastoma cells, Anal. Chem. 92 (11) (2020) 7746–7753.
- [35] A.-Y. Chang, X. Liu, Y. Pei, C. Gong, P.U. Arumugam, S. Wang, Dopamine sensing with robust carbon nanotube implanted polymer micropillar array electrodes fabricated by coupling micromolding and infiltration coating processes, Electrochim. Acta 368 (2021) 137632.
- [36] P.C.W. Fung, R.K.C. Kong, The integrative five-fluid circulation system in the human body, Open J. Mol. Integr. Physiol. 6 (04) (2016) 45.
- [37] N.Y. Kim, H.Y. Lee, Y.Y. Choi, S.J. Mo, S. Jeon, J.H. Ha, S.D. Park, J.-J. Shim, J. Lee, B.G. Chung, Effect of gut microbiota-derived metabolites and extracellular vesicles on neurodegenerative disease in a gut-brain axis chip, Nano Convergence 11 (1) (2024) 1–13.
- [38] A.E. Wheeler, V. Stoeger, R.M. Owens, Lab-on-chip technologies for exploring the gut-immune axis in metabolic disease, Lab Chip (2024).
- [39] R.M. Wightman, L.J. May, A.C. Michael, Detection of dopamine dynamics in the brain, Anal. Chem. 60 (13) (1988) 769A–A793.
- [40] M. Senel, E. Dervisevic, S. Alhassen, M. Dervisevic, A. Alachkar, V.J. Cadarso, N. H. Voelcker, Microfluidic electrochemical sensor for cerebrospinal fluid and blood dopamine detection in a mouse model of Parkinson's disease, Anal. Chem. 92 (18) (2020) 12347–12355.
- [41] S. Mao, C. Fonder, M.F. Rubby, G.J. Phillips, D.S. Sakaguchi, L. Que, An integrated microfluidic chip for studying the effects of neurotransmitters on neurospheroids, Lab Chip 23 (6) (2023) 1649–1663.
- [42] S. Mao, C. Fonder, F. Rubby, R. Yang, G. Phillips, D. Sakaguchi, L. Que, A Microchip For Studying the Effects of Dopamine and its Precursor On Neurospheroids, in: 2022 IEEE 35th International Conference on Micro Electro Mechanical Systems Conference (MEMS), IEEE, 2022, pp. 305–308.
- [43] C. Spegel, A. Heiskanen, L.H.D. Skjolding, J. Emnéus, Chip based electroanalytical systems for cell analysis, Electroanalysis 20 (6) (2008) 680–702.

- [44] R.F. Lane, A.T. Hubbard, Differential double pulse voltammetry at chemically modified platinum electrodes for in vivo determination of catechol amines, Anal. Chem. 48 (9) (1976) 1287–1293.
- [45] A.D.I. Aliagan, M.D. Ahwazi, N. Tombo, Y. Feng, J.C. Bopassa, Parkin interacts with Mitofilin to increase dopaminergic neuron death in response to Parkinson's disease-related stressors, Am. J. Transl. Res. 12 (11) (2020) 7542.
- [46] L. Gao, W. Zhou, B. Symmes, C.R. Freed, Re-cloning the N27 dopamine cell line to improve a cell culture model of Parkinson's disease, PLoS One 11 (8) (2016) e0160847.
- [47] X. Ding, M.F. Rubby, S. Que, S. Uchayash, L. Que, Facile Process for Fabrication of Silicon Micro-Nanostructures of Different Shapes as Molds for Fabricating Flexible Micro-Nanostructures and Wearable Sensors, ACS Appl. Mater. Interfaces 15 (9) (2023) 12202–12208.
- [48] Y. He, X. Che, L. Que, A top-down fabrication process for vertical hollow silicon nanopillars, J. Microelectromech. Syst. 25 (4) (2016) 662–667.
- [49] A. Villa, I. Liste, E.T. Courtois, E.G. Seiz, M. Ramos, M. Meyer, B. Juliusson, P. Kusk, A. Martinez-Serrano, Generation and properties of a new human ventral mesencephalic neural stem cell line, Exp. Cell Res. 315 (11) (2009) 1860–1874.
- [50] M. Pravda, J.M. Kauffmann, Y. Michotte, Development of an On-Line Electrochemical Biosensor for Glucose Determination in Rat Brain Using Microdialysis Sampling, Electroanalysis 12 (12) (2000) 912–916.
- [51] X. Chen, H. Wan, R. Guo, X. Wang, Y. Wang, C. Jiao, K. Sun, L. Hu, A double-layered liquid metal-based electrochemical sensing system on fabric as a wearable detector for glucose in sweat, Microsyst. Nanoeng, 8 (1) (2022) 48.
- [52] R. Yang, J. Boldrey, D. Jiles, I. Schneider, L. Que, On chip detection of glial cell-derived neurotrophic factor secreted from dopaminergic cells under magnetic stimulation, Biosens. Bioelectron. 182 (2021) 113179.
- [53] C. Chaparro, L. Herrera, A. Meléndez, D. Miranda, Considerations on electrical impedance measurements of electrolyte solutions in a four-electrode cell, J. Phys.: Conf. Ser. (2016) 012101.

- [54] H.-F. Tsai, J.-Y. Cheng, H.-F. Chang, T. Yamamoto, A.Q. Shen, Uniform electric field generation in circular multi-well culture plates using polymeric inserts, Sci. Rep. 6 (1) (2016) 26222.
- [55] A.J. Steckl, P. Ray, Stress biomarkers in biological fluids and their point-of-use detection, ACS Sensors 3 (10) (2018) 2025–2044.
- [56] S. Sandeep, A.S. Santhosh, N.K. Swamy, G.S. Suresh, J.S. Melo, K.S. Nithin, Electrochemical detection of L-dopa using crude Polyphenol oxidase enzyme immobilized on electrochemically reduced RGO-Ag nanocomposite modified graphite electrode, Mater. Sci. Eng. B 232 (2018) 15–21.
- [57] V. Ratautaite, U. Samukaite-Bubniene, D. Plausinaitis, R. Boguzaite, D. Balciunas, A. Ramanaviciene, G. Neunert, A. Ramanavicius, Molecular imprinting technology for determination of uric acid, Int. J. Mol. Sci. 22 (9) (2021) 5032.
- [58] S. Rantataro, L. Ferrer Pascual, T. Laurila, Ascorbic acid does not necessarily interfere with the electrochemical detection of dopamine, Sci. Rep. 12 (1) (2022) 20225
- [59] C. Kavitha, K. Bramhaiah, N.S. John, Low-cost electrochemical detection of L-tyrosine using an rGO–Cu modified pencil graphite electrode and its surface orientation on a Ag electrode using an ex situ spectroelectrochemical method, RSC Adv. 10 (39) (2020) 22871–22880.
- [60] Y.-F. Hu, Z.-H. Zhang, H.-B. Zhang, L.-J. Luo, S.-Z. Yao, Electrochemical determination of l-phenylalanine at polyaniline modified carbon electrode based on β-cyclodextrin incorporated carbon nanotube composite material and imprinted sol–gel film, Talanta 84 (2) (2011) 305–313.
- [61] J.-J. Xu, C. Wang, H.-Y. Chen, Electrochemical characteristics of nickel hexacyanoferrate monolayer anchoring to Bi-(2-aminoethyl)-aminodithiocarboxyl acid self-assembled film modified electode, Anal. Sci. 16 (2) (2000) 231–234.
- [62] S. Chumillas, M.C. Figueiredo, V. Climent, J.M. Feliu, Study of dopamine reactivity on platinum single crystal electrode surfaces, Electrochim. Acta 109 (2013) 577, 586